Mon. Not. R. Astron. Soc. **000**, 000–000 (0000) Printed 18 February 2015 (MN LaTeX style file v2.2)

Massive stars exploding in a He-rich circumstellar medium. V. Observations of the slow-evolving SN Ibn OGLE-2012-SN-006

A. Pastorello,[1]⋆ Ł. Wyrzykowski,[2,3] S. Valenti,[4,5] J. L. Prieto,[6,7] S. Kozłowski,[2] A. Udalski,[2] N. Elias-Rosa,[1] A. Morales-Garoffolo,[8] J. P. Anderson,[9] S. Benetti,[1] M. Bersten,[10,11,12] M. T. Botticella,[13] E. Cappellaro,[1] G. Fasano,[1] M. Fraser,[14] A. Gal-Yam,[15] M. Gillone,[16] M. L. Graham,[4,5] J. Greiner,[17] S. Hachinger,[18,1] D. A. Howell,[4,5] C. Inserra,[19] J. Parrent,[4,20] A. Rau,[17] S. Schulze,[7,21] S. J. Smartt,[19] K. W. Smith,[19] M. Turatto,[1] O. Yaron,[15] D. R. Young,[19] M. Kubiak,[2] M. K. Szymański,[2] G. Pietrzyński,[2,22] I. Soszyński,[2] K. Ulaczyk,[2] R. Poleski,[2,23] P. Pietrukowicz,[2] J. Skowron,[2] and P. Mróz.[2]

[1] *INAF - Osservatorio Astronomico di Padova, Vicolo dell' Osservatorio 5, 35122 Padova, Italy*
[2] *Warsaw University Observatory, Al. Ujazdowskie 4, 00-478 Warszawa, Poland*
[3] *Institute of Astronomy, University of Cambridge, Madingley Road, Cambridge CB3 0HA, UK*
[4] *Las Cumbres Observatory Global Telescope Network, Inc. Santa Barbara, CA 93117, USA*
[5] *Department of Physics, University of California Santa Barbara, Santa Barbara, CA 93106-9530, USA*
[6] *Núcleo de Astronomía de la Facultad de Ingeniería, Universidad Diego Portales, Av. Ejército 441, Santiago, Chile*
[7] *Millennium Institute of Astrophysics, Santiago, Chile*
[8] *Institut de Ciències de l'Espai (CSIC-IEEC), Campus UAB, Torre C5, 2a planta, 08193 Barcelona, Spain*
[9] *European Southern Observatory, Alonso de Cordova 3107, Vitacura, Santiago, Chile*
[10] *Instituto de Astrofísica La Plata, IALP (CCT La Plata), CONICET-UNLP, Paseo del Bosque s/n, 1900 La Plata, Argentina*
[11] *Facultad de Ciencias Astronómicas y Geofísicas, Universidad Nacional de La Plata, Paseo del Bosque s/n, 1900 La Plata, Argentina*
[12] *Kavli Institute for the Physics and Mathematics of the Universe (WPI), The University of Tokyo, Kashiwa, Chiba 277-8583, Japan*
[13] *INAF Osservatorio Astronomico di Capodimonte, Salita Moiariello, 16 80131 Napoli, Italy*
[14] *Institute of Astronomy, University of Cambridge, Madingley Road, Cambridge CB3 0HA, UK*
[15] *Department of Particle Physics and Astrophysics, Faculty of Physics, The Weizmann Institute of Science, Rehovot 76100, Israel*
[16] *School of Physics and Astronomy, University of Birmingham, Edgbaston, Birmingham B15 2TT, UK*
[17] *Max-Planck-Institut für extraterrestrische Physik, Giessenbachstrasse 1, 85748 Garching, Germany*
[18] *Institut für Theoretische Physik und Astrophysik, Universität Würzburg, Emil-Fischer-Str. 31, 97074 Würzburg, Germany*
[19] *Astrophysics Research Centre, School of Mathematics and Physics, Queen's University Belfast, Belfast BT7 1NN, UK*
[20] *6127 Wilder Lab, Department of Physics & Astronomy, Dartmouth College, Hanover, NH 03755, USA*
[21] *Instituto de Astrofísica, Facultad de Física, Pontificia Universidad Católica de Chile, 306, Santiago 22, Chile*
[22] *Departamento de Física, Universidad de Concepción, Casilla 160-C, Concepción, Chile*
[23] *Department of Astronomy, Ohio State University, 140 West 18th Avenue, Columbus, OH 43210, USA*

Accepted XXXX Month XX. Received XXXX Month XX; in original form XXXX Month XX

ABSTRACT

We present optical observations of the peculiar Type Ibn supernova (SN Ibn) OGLE-2012-SN-006, discovered and monitored by the $OGLE-IV$ survey, and spectroscopically followed by $PESSTO$ at late phases. Stringent pre-discovery limits constrain the explosion epoch with fair precision to JD = 2456203.8 ± 4.0. The rise time to the I-band light curve maximum is about two weeks. The object reaches the peak absolute magnitude $M_I = -19.65 \pm 0.19$ on $JD = 2456218.1 \pm 1.8$. After maximum, the light curve declines for about 25 days with a rate of 4 mag 100d^{-1}. The symmetric I-band peak resembles that of canonical Type Ib/c supernovae (SNe), whereas SNe Ibn usually exhibit asymmetric and narrower early-time light curves. Since 25 days past maximum, the light curve flattens with a decline rate slower than that of the ^{56}Co to ^{56}Fe decay, although at very late phases it steepens to approach that rate. However, other observables suggest that the match with the ^{56}Co decay rate is a mere coincidence, and the radioactive decay is not the main mechanism powering the light curve of OGLE-2012-SN-006. An early-time spectrum is dominated by a blue continuum, with only a marginal evidence for the presence of He I lines marking this SN Type. This spectrum shows broad absorptions bluewards than 5000Å, likely O II lines, which are similar to spectral features observed in super-luminous SNe at early epochs. The object has been spectroscopically monitored by $PESSTO$ from 90 to 180 days after peak, and these spectra show the typical features observed in a number of SN 2006jc-like events, including a blue spectral energy distribution and prominent and narrow ($v_{FWHM} \approx 1900$ km s^{-1}) He I emission lines. This suggests that the ejecta are interacting with He-rich circumstellar material. The detection of broad (10^4 km s^{-1}) O I and Ca II features likely produced in the SN ejecta (including the [O I] $\lambda\lambda$6300,6364 doublet in the latest spectra) lends support to the interpretation of OGLE-2012-SN-006 as a core-collapse event.

Key words: supernovae: general — supernovae: individual (OGLE-2012-SN-006, SN 2006jc, SN 2010al)

1 INTRODUCTION

Supernovae of Type Ibn (SNe Ibn) are considered a rare group of stripped-envelope core-collapse (CC) events which interact with H-depleted circumstellar material (CSM). The spectra of SNe Ibn are characterized by relatively narrow lines of He I in emission (hence the designation as “Ibn”, Pastorello et al. 2008a), with full-width at half maximum (FWHM) velocities ranging from several hundreds to a few thousands km s^{-1}. These features are thought to arise in the interactions between the SN ejecta and He-rich (and H-poor) CSM. However, weak H lines have been occasionally detected in the spectra of a few Type Ibn SNe, suggesting the presence of residual H in the CSM of -at least- a sub-sample of SNe Ibn (Pastorello et al. 2008b; Smith et al. 2012; Pastorello et al. 2015a).

The prototype of this family, SN 2006jc, has been associated with a precursor eruptive episode which occurred a couple of years before the SN explosion and reached a peak absolute magnitude $M_R \approx$ -14 (Yamaoka et al. 2006; Nakano et al. 2006; Pastorello et al. 2007; Foley et al. 2007). SN 2006jc, although discovered after the maximum light, was widely studied. The brightest magnitude registered for this SN was M_R = -18.3 (Pastorello et al. 2007), and its optical light curve experienced a rapid post-peak decline (about 3.5 mag during the first 50 days after discovery). At later phases, the increasing decline rate of the optical light curve and the simultaneous near-infrared (NIR) excess were explained as the consequence of dust forming in a cool dense shell (e.g. Smith et al. 2008; Mattila et al. 2008). Tominaga et al. (2008) and Pastorello et al. (2008b) attempted to reproduce the evolution of SN 2006jc with radioactively powered models. They both favoured models with a high kinetic energy (E$_k \sim 10^{52}$ erg), and moderate masses of ejecta (M$_{ej} \approx$ 4.5-5 M$_\odot$) and synthesized ^{56}Ni (M$_{^{56}Ni} \approx$ 0.2-0.25 M$_\odot$). Nonetheless, radioactively powered models with even lower E$_k$ and M$_{ej}$ provided decent matches with observations (e.g., models A and B in Pastorello et al. 2008b, were obtained adopting the following parameters: E$_k \sim 10^{51}$ erg, M$_{ej} \leqslant$ 1 M$_\odot$ and M$_{^{56}Ni} \sim$ 0.25-0.40 M$_\odot$). On the other hand, Chugai (2009) showed that radioactive models with modest M$_{ej}$/M$_{^{56}Ni}$ ratio were unrealistic for a Type Ib/c SN explosion, and proposed that the observed parameters of SN 2006jc were best explained with strong ejecta-CSM interaction occurring already at early phases. In fact, the interaction with a circumstellar shell with mass of a few hundredths M$_\odot$ would fairly well explain the properties of SN 2006jc. It is clear, however, that for an accurate modelling good data coverage is essential along the duration of the entire SN evolution, including the very early phases, not available for SN 2006jc. The first opportunity to study a SN Ibn soon after its explosion was offered by SN 2010al, which initially showed an almost featureless spectrum with the shape of a hot blackbody (the data of this object are presented in Pastorello et al. 2015a).

The proliferation of well-organized imaging surveys,

⋆ andrea.pastorello@oapd.inaf.it

with different depths and strategies, has significantly increased the number of transients discovered and, hence, the number of Type Ibn candidates. The *Optical Gravitational Lensing Experiment* (*OGLE*, Udalski et al. 1997) is a long-term project carried out initially with the 1-m Swope telescope, and later with the 1.3-m Warsaw University Telescope, both located at the Las Campanas Observatory (Chile). The fields monitored in the course of the different seasons of the search included the two Magellanic Clouds and the Magellanic Bridge.[1] In the current fourth season ($OGLE-IV$, Wyrzykowski et al. 2014), which started in 2009, the survey is making use of a 32 CCD mosaic camera covering a field of 1.4 square degrees and equipped with V and I filters. Originally conceived to study microlensing events (Paczynski 1986, 1991), a by-product of the project is the discovery of a huge number of transients and variable stars of all types, including SNe (Kozlowski et al. 2013).

The study of new types of stellar explosions is the main goal of the *"Public ESO Spectroscopic Survey of Transient Objects"* ($PESSTO$,[2] see Smartt et al. 2013), which is a public spectroscopic survey running at the 3.58-m New Technology Telescope (NTT) of the European Southern Observatory (ESO) in La Silla (Chile). The survey is planned for four years (starting from April 2012) and is operative 90 nights per year. The survey aims to classify a large number of transients and to monitor the most interesting objects with EFOSC2 (optical) and SOFI (near-infrared). Priority $PESSTO$ targets are the most unusual SNe, SN impostors or very nearby transients, for which detailed high-quality, multi-wavelength observational campaigns can be arranged.

A specific subproject has been defined within $PESSTO$ in order to study SNe Ibn (Pastorello et al. 2008a). Two Type Ibn SNe discovered by the $LaSilla-QUEST$ variability survey and followed by $PESSTO$ (LSQ12btw and LSQ13ccw), are studied in a companion paper to the present work (Pastorello et al. 2015b). A few months after LSQ12btw, a new SN Ibn candidate, OGLE-2012-SN-006, was discovered in the course of the $OGLE-IV$ survey (Wyrzykowski et al. 2012, 2014). The object has coordinates $RA = 3^h33^m34^s.79$ and $Dec = -74^o23'40''.1$ (J2000), and lies in a faint, anonymous host galaxy (Figure 1). According to Wyrzykowski et al. (2012), the object had a magnitude $I = 17.62$ at maximum light. OGLE-2012-SN-006 was spectroscopically classified on 2013 January 10.2 UT by Prieto & Morrell (2013) as a Type Ibn SN, similar to SN 2006jc. The host galaxy redshift, as estimated from the position of the narrow SN features, is z = 0.057± 0.001. Adopting a Hubble constant value of $H_0 = 73 \pm 5$ km s^{-1} Mpc^{-1} ($\Omega_m = 0.27$, and $\Omega_\Lambda = 0.73$), we obtain a luminosity distance of 244.5 ± 20.0 Mpc.

Pastorello et al. (2008a), on the basis of a very small sample of objects, proposed that SNe Ibn might form a relatively homogeneous group of mildly interacting stripped-envelope SNe. However, recent discoveries suggest that SNe Ibn span a much wider range of properties than initially believed (Smith et al. 2012; Gorbikov et al. 2014; Sanders et al. 2013; Pastorello et al. 2015a,b). In this context, because of its slow evolving light curve (see Section 2.1), OGLE-2012-SN-006 can be considered as an unprecedented addition to the Type Ibn SN zoo.

2 OBSERVATIONS

Our photometric and spectroscopic data have been reduced using standard procedures in the IRAF environment.[3]

Optical imaging frames were first pre-reduced (i.e. overscan, bias and flat-field corrected, and trimmed in order to remove the unexposed regions of the image). In the near-infrared (NIR) photometry images we also removed the contribution of the bright NIR background from the science images. Sky images were obtained by median-combining a number of dithered science frames, and were finally subtracted from each science image. In order to improve the signal to noise, the sky-subtracted science images were spatially registered and finally combined.

Photometric measurements in the optical and NIR bands were obtained through the PSF-fitting technique. A template PSF was built using stars in the SN field. With this PSF model along with a low-order polynomial surface, we finally performed a fit to the SN and the underlying background. $OGLE-IV$ photometry was obtained using the Difference Imaging Analysis (DIA), which is a template subtraction method adapted to the $OGLE$ data and detailed in Wyrzykowski et al. (2014) (see also Wozniak 2000). The magnitudes of several stars in the SN field (see Figure 1, left) were calibrated using observations of standard fields of the Landolt (1992) catalogue. The magnitudes obtained in photometric nights were used to estimate reliable average magnitudes for the entire local stellar sequence (23 stars), which was finally used for the calibration of the SN photometry obtained during non-photometric nights.

The NIR SN photometry was calibrated through a comparison with 14 stars of the optical sequence for which NIR magnitudes were available in the The Two Micron All Sky Survey (2MASS) catalogue (Skrutskie et al. 2006). The optical and NIR magnitudes of the SN are reported in Tables A1 and A2, while those of the local sequence stars are in Table A3.

The pre-reduction process of optical spectroscopy frames followed the steps described above for photometric frames. Then, one-dimensional spectra were optimally extracted in IRAF, and wavelength calibrated using reference spectra of arc lamps. Finally, sensitivity curves obtained using spectra of spectro-photometric standards allowed us to flux-calibrate the SN spectra. Telluric absorption features were removed using normalized telluric absorption profiles derived from the spectrum of the standard star.

For the NIR spectra, two additional steps were required: firstly, we had to remove the intense background emission. This was achieved through the subtraction of two consecutive exposures (one from the other), since during the observation the source was dithered along the slit direction. Secondly, we used spectra of telluric standard stars to remove

---

[1] A few additional fields were monitored by *OGLE* in the Galactic bulge and disk.

[2] *http://www.pessto.org*

[3] IRAF is distributed by the National Optical Astronomy Observatory, which is operated by the Association of Universities for Research in Astronomy (AURA) under cooperative agreement with the National Science Foundation.

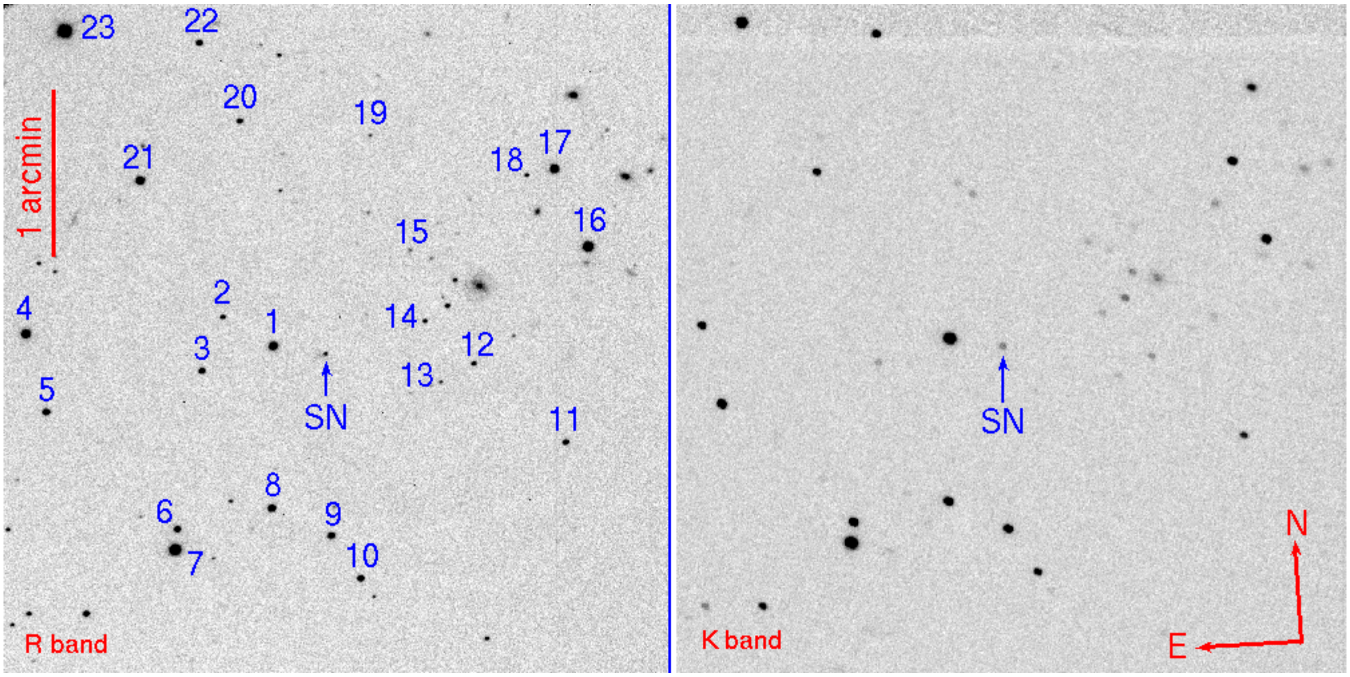

Figure 1. Left: ESO-NTT EFOSC2 $R-$band image of OGLE-2012-SN-006 obtained on January 19, 2013; the numbers mark the reference stars used to calibrate the SN magnitude. Right: ESO-NTT SOFI $Ks-$band image of OGLE-2012-SN-006 obtained on January 21, 2013.

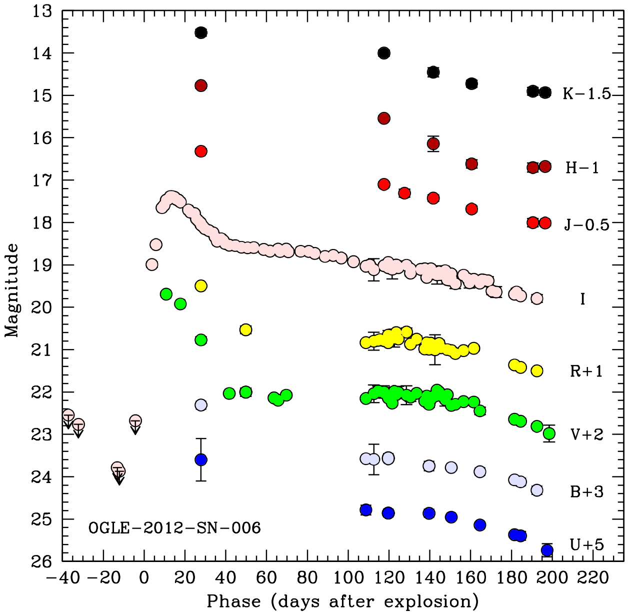

Figure 2. Optical and NIR light curves of OGLE-2012-SN-006. The light curves are shifted by the same amount indicated by the labels to the right. The phase axis is computed in days since explosion (JD = 2456203.8 ± 4.0).

the very broad (typically saturated in the NIR) atmospheric absorption bands.

Finally, the consistency of the spectroscopic flux calibration in the optical and NIR spectra was checked with available SN magnitudes and, in case of a discrepancy, the spectral fluxes were rescaled to the photometry. The log of spectroscopic observations of OGLE-2012-SN-006 is reported in Table 1. The spectroscopic data of OGLE-2012-SN-006 are available from the ESO archive as PESSTO Phase 3 data products (see *http://www.pessto.org*) and are also available via WISeREP (Yaron & Gal-Yam 2012).[4]

2.1 Analysis of the Light Curves

Routine $I-$band observations of the $OGLE - IV$ fields resulted in an excellent monitoring of the region where OGLE-2012-SN-006 exploded. $OGLE - IV$ observations (Wyrzykowski et al. 2014) of the SN field were collected since early July 2012, and the last non-detection was registered on 2012 September 29.26 UT. The first detection of OGLE-2012-SN-006 was on 2012 October 7.34 UT, so we can constrain the explosion epoch with a relatively small uncertainty to 2012 October 3.30 UT (JD = 2456203.8 ± 4.0). After discovery, the object showed a relatively fast light curve rise to $I-$band maximum, lasting $\sim$ 2 weeks from the adopted explosion time. Using a low-order polynomial fit to the data, we estimated the magnitude of the $I-$band light curve maximum to be $I = 17.41 \pm 0.02$ (on 2012 October 17.6 UT, i.e. JD = 2456218.1 ± 1.8). Adopting a distance modulus of $\mu = 36.94 \pm 0.19$ mag for the galaxy hosting OGLE-2012-SN-006 (see Section 1), assuming negligible host galaxy

---

[4] We note that the data presented and analysed in this paper were custom reduced, and not obtained from the First Release of *PESSTO* Spectral data products (SSDR1). This is because the analysis was performed before *PESSTO* SSDR1, and the faintness of the object required a careful treatment.

reddening[5] and a Galactic contribution to the total extinction of $A_I = 0.12$ mag (obtained adopting the dust map calibration of Schlafly & Finkbeiner 2011), we obtain an absolute magnitude at peak of M_I = -19.65 ± 0.19. After maximum, the $I-$band light curve experienced a relatively fast decline (with a slope of $\gamma_1 \approx 4$ mag 100d^{-1}) lasting about 25 days, followed by a flattening from +25 days to +70 days past maximum ($\gamma_2 \approx 0.40$ mag 100d^{-1}). Such an optical/NIR flattening, making the magnitude decline rate slower than expected for a SN powered by radioactivity of ^{56}Co, has never been observed in any SN Ibn. After that, the I-band light curve becomes slightly steeper ($\gamma_3 \approx 0.74$ mag 100d^{-1}), showing a slope which is closer to ^{56}Co decay (0.98 mag 100d^{-1}), but still slightly flatter than that slope. A similar decline rate in the late-time luminosity is measured in all optical bands. We note that the relatively slow late-time decline of OGLE-2012-SN-006 looks also alike that observed in some H-rich interacting SNe, such as the Type IIn SN 2010jl (see below). The increased slope of the I-band light curve at very late phases is confirmed by a very late detection on 2013 August 1st, and by deep detection limits at later epochs. This is possibly an indication of dust formation at very late phases. We note that spectroscopic indicators also support this claim (see Section 2.2).

During early phases, the evolution of OGLE-2012-SN-006 was poorly monitored in the other bands. The object was occasionally observed in the V-band by the $OGLE-IV$ survey, as well as in the g', r', i' Sloan bands[6] and in the near-infrared (NIR) with the 2.2-m MPI/ESO Telescope in La Silla equipped with GROND (Greiner et al. 2008). However, after the SN classification, we realized that this was the first opportunity to monitor a Type Ibn SN until very late phases, since the object was showing a very slow photometric evolution. Therefore we increased the monitoring frequency of the $PESSTO$ campaign in the optical and NIR bands using the NTT equipped with EFOSC2 and SOFI, and the 1-m LCOGT Telescope located at Cerro Tololo Inter-American Observatory (CTIO). This late-time monitoring allowed us to follow in detail the late evolution of OGLE-2012-SN-006, to compute its quasi-bolometric light curve and eventually put an upper limit to the ^{56}Ni mass.

In Figure 3 (top) the I-band absolute light curve of OGLE-2012-SN-006 is compared with those of SNe 2006jc, 2010al and 2010jl (the latter being a Type IIn event). For SN 2006jc we adopted $\mu = 32.01$ mag, $A_{I,tot} = 0.03$ mag and JD(max) = 2454008, for SN 2010al $\mu = 34.25$ mag, $A_{I,tot}$ = 0.10 mag and JD(max) = 2455285, while for SN 2010jl μ = 33.45 mag, $A_{I,tot} = 0.09$ mag and JD(I,max) = 2455494. The distance and the reddening adopted for OGLE-2012-SN-006 are those discussed above. For SN 2010al the best monitored R-band light curve is also shown as a comparison. OGLE-2012-SN-006 is significantly brighter than the other two SNe Ibn during its entire evolution (though fainter than SN 2010jl). We note that the early post-peak luminosity declines of SNe 2010al and 2006jc are similar, whilst OGLE-2012-SN-006 flattens quite early (at phase ∼ 25-30 days past maximum). However, the late-time photometric behaviour of SN 2006jc (and, possibly, SN 2010al) is mostly determined by dust formation which produces a flux deficit in the optical and an enhanced emission in the infrared domain (Smith et al. 2008; Mattila et al. 2008; Pastorello et al. 2015a). Clearly, this was not observed in OGLE-2012-SN-006. We also note that the decline rate of the I-band light curve of OGLE-2012-SN-006 at phases later than ∼25 days after maximum is similar to that of the the Type IIn SN 2010jl, which showed unequivocal evidence of ejecta-CSM interaction at all evolutionary stages.

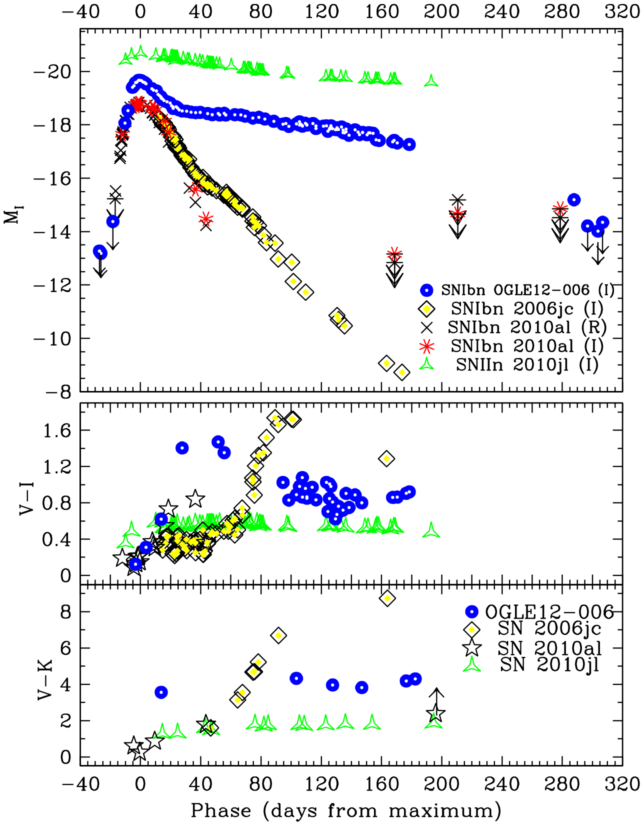

Figure 3. Comparisons of the I-band absolute light curves (top), $V-I$ (middle) and $V-K$ (bottom) colour curves of SNe OGLE-2012-SN-006, 2010al, 2006jc and the Type IIn SN 2010jl. Data of SN 2010al are from Pastorello et al. (2015a), those of SN 2006jc are from Pastorello et al. (2007, 2008b); Foley et al. (2007); Mattila et al. (2008); Di Carlo et al. (2008); Anupama et al. (2009) and those of SN 2010jl are from Stoll et al. (2011); Zhang et al. (2012); Fransson et al. (2014). In the top panel, together with the I-band light curves of the SN sample, the well-followed R-band light curve of SN 2010al has been included.

In the middle panel of Figure 3, the $V-I$ colour curves of the above-mentioned objects are shown. We note that OGLE-2012-SN-006 becomes red very rapidly, moving from a blue colour at early stages to $V-I \approx 1.4$ mag at about 30 days after maximum. Then the $V-I$ colour turns slightly

---

[5] From the earliest spectrum (see Section 2.2), we do not see any clear signature of the narrow interstellar Na I doublet (Na ID) at the parent galaxy redshift, suggesting little (if any) contribution of the host galaxy to the total reddening of OGLE-2012-SN-006.

[6] Sloan g', r', i' magnitudes were transformed into Johnson B, V, R and I magnitudes following the prescriptions reported in *http://www.mpe.mpg.de/~jcg/GROND/calibration.html.*

Table 1. Log of the spectroscopic observations of OGLE-2012-SN-006.

Date	JD-2400000	Days since maximum	Instrumental configuration	Range (Å)	Resolution (Å)
Oct 15, 2012	56215.81	-2.3	DuPont+B&C	3600-10000	27
Jan 10, 2013	56302.70	+84.6	DuPont+WFCCD	3750-9190	8
Jan 20, 2013	56312.56	+94.5	NTT+EFOSC2+gm11+gm16	3360-10090	14;14
Feb 20, 2013	56343.68	+125.6	NTT+EFOSC2+gm13	3680-9300	18
Feb 22, 2013	56345.64	+127.5	NTT+SOFI+Blue+Red	9360-25000	24;32
Mar 18, 2013	56369.64	+151.5	NTT+EFOSC2+gm13	3650-9300	18
Apr 19, 2013	56402.49	+184.4	NTT+EFOSC2+gm13	3660-9280	18

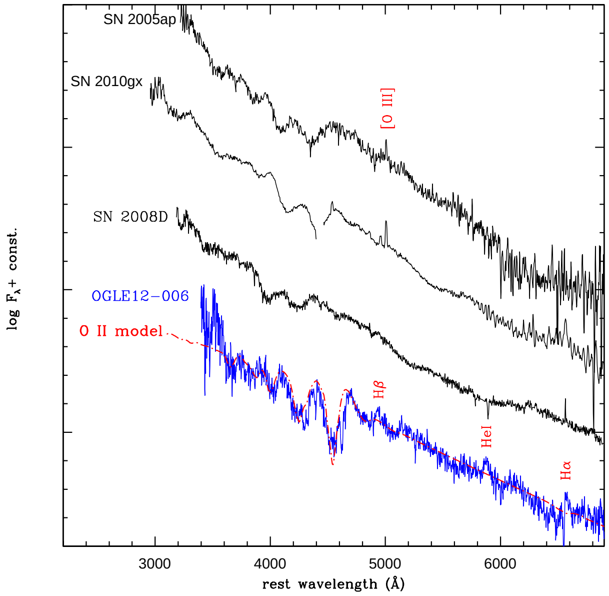

Figure 4. Comparison of our earliest spectrum of OGLE-2012-SN-006 (phase = -2.4 days from maximum) with pre-maximum spectra of other stripped envelope SNe. Our sample includes the super-luminous SNe 2005ap (Quimby et al. 2007, phase = -3.6 days from maximum) and 2010gx (Pastorello et al. 2010, time dilation corrected phase = -4.3 days from maximum), and a spectrum of the Type Ib SN 2008D obtained soon after the shock breakout (Modjaz et al. 2009, i.e. about 1.8 days after the X-ray burst, and -16.6 days from the V-band maximum). A *SYNOW* model, labelled as "O II model", is overplotted to the observed spectrum of OGLE-2012-SN-006. The model was obtained adopting a continuum temperature of 11000 K, a photospheric velocity of 7000 km s^{-1}, and including a single contributing species, O II.

bluer in the following couple of months, and thereafter settles to about 0.8 mag. The evolution of the $V-I$ colour in SN 2006jc is quite different, since it remains almost constant (0.3-0.4 mag) until ∼50 days. Later on, it rapidly rises to $V-I \approx 1.6$ mag up to day 90, and finally declines to 1.2 mag at about 160 days. Unfortunately, for SN 2010al, the $V-I$ colour monitoring was limited only at the early phases (Pastorello et al. 2015a). However, from the available data, the evolution of the three SNe is substantially similar until day ∼20.

The bottom panel of Figure 3 shows the $V-K$ colour evolution. Whilst the $V-K$ colour in OGLE-2012-SN-006 remains roughly constant over the entire monitored evolution ($V-K \approx 4$ mag, ranging from 3.5 mag at early phases to 4.3 mag at late phases), the $V-K$ colour of SN 2006jc shows a monotonic rise from ∼1.4 mag at 1.5 months after maximum to ∼8.8 mag at day 160. Again, the $V-K$ colour of SN 2010al is available only at early phases (from around the light curve peak to 1.5 months after), and - in terms of time evolution - apparently mimics that of SN 2006jc. We note that colours of the SN IIn 2010jl evolve very little during the first 6 months of its evolution, and remain quite blue.

2.2 Spectral Evolution

The object was discovered at very early stages, and the first spectrum (2012 October 15; Figure 4), dominated by a blue, almost featureless continuum, did not allow a secure classification of the object. The temperature as obtained from a blackbody fit to the spectral continuum is 11000 ± 1200 K. Weak lines of He I λ5876, Hα and Hβ are detected. A number of broad absorption features are visible at wavelengths shorter than 5000 Å. These absorptions somewhat resemble the O II features observed in spectra of super-luminous stripped envelope SNe (such as SNe 2005ap and 2010gx, see Figure 4, Quimby et al. 2011; Pastorello et al. 2010) or even the putative higher ionization CNO lines detected by Modjaz et al. (2009) in the earliest spectrum of the more canonical Type Ib SN 2008D. In order to identify the lines in this early spectrum, we computed a model using the spectral synthesis code *SYNOW* (Fisher 2000). We adopt a continuum temperature of 11000 K and a velocity at the photosphere of 7000 km s^{-1}, which is significantly lower (by a factor 2 to 3) than those measured in the comparison objects of Figure 4. The contribution of O II alone is sufficient to reproduce most spectral features in the wavelengths range between 3500 Å and 5000 Å. We find a good match between our synthetic *SYNOW* spectrum and the observed one, making the identification of the spectral features as O II quite robust. However, we cannot rule out a contribution from other CNO ions, including N III, to shape the observed features in the October 15 spectrum of OGLE-2012-SN-006.

Another spectrum was obtained on 2013 January 10, and allowed Prieto & Morrell (2013) to classify the object as a Type Ibn SN because of the presence of strong, narrow He I lines in emission. These first two spectra of our sequence were both obtained with the 2.5-m DuPont Telescope at the Las Campanas Observatory (LCO), the former using a B&C spectrograph, the latter with WFCCD. After the classification announcement, i.e. when the object was ∼3 months old, we started a continuous (though relaxed) *PESSTO* moni-

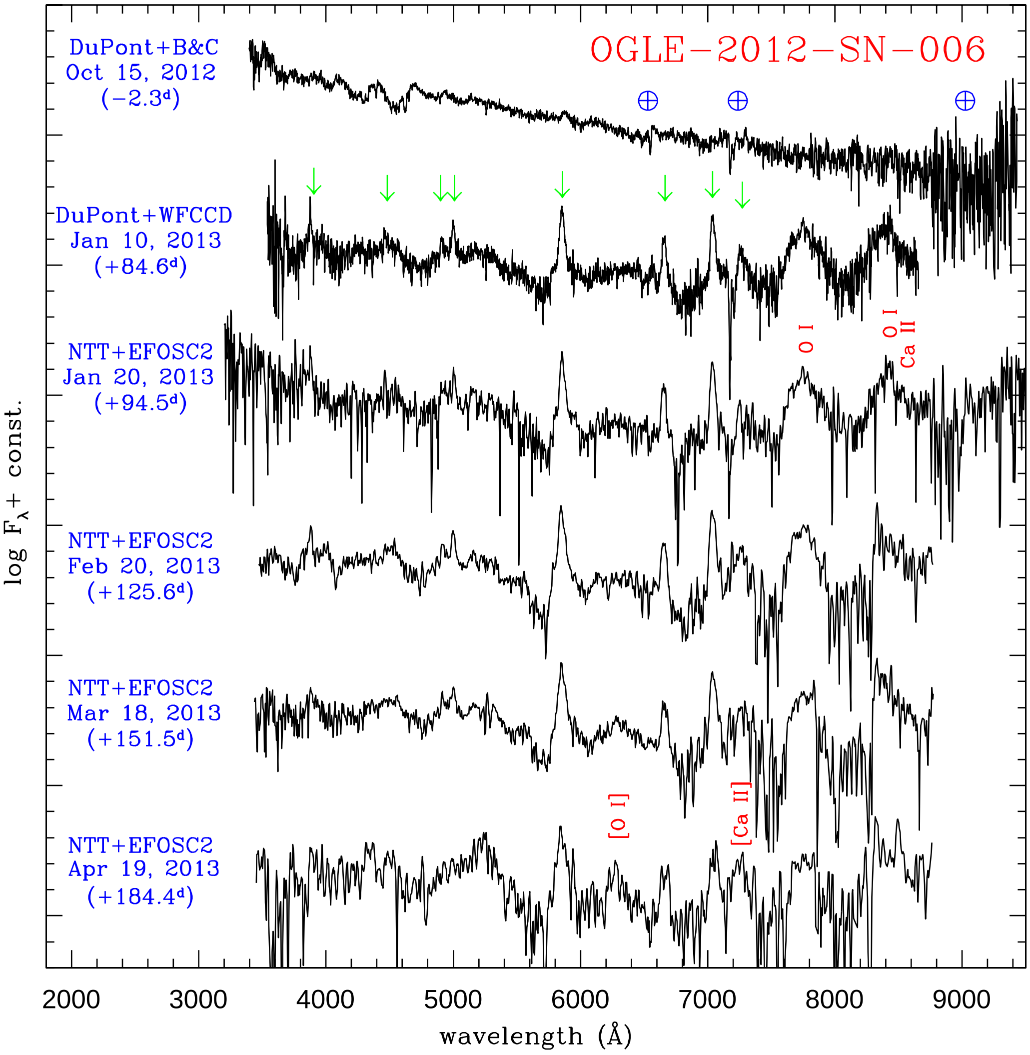

Figure 5. Sequence of optical spectra of OGLE-2012-SN-006 reported at the rest wavelength frame. The positions of the strongest He I lines are marked with green arrows. The most important SN nebular lines are also labelled. The positions of the most prominent telluric features are marked with the "⊕" symbol. The phases reported in parenthesis are days from the maximum light.

toring campaign using the NTT (with EFOSC2 and SOFI). Our complete spectral sequence is shown in Figure 5.

The optical spectra obtained in January and February 2013 display very little evolution. They show a blue spectral energy distribution (SED), with a clear flux attenuation at wavelengths longer than about 5600 Å. The blue SED is a common property of Type Ibn SNe as well as other interacting events, and is possibly generated by blends of Fe emission lines (e.g. Smith et al. 2009). A very broad absorption feature, with a FWHM ∼ 270 Å, is detected at about 4800 Å. This is a common feature in SNe Ibn, and is probably due to Fe II lines. Much narrower He I lines are clearly detected in emission with a $v_{FWHM} \approx 1300$ km s^{-1}. The strongest line at optical wavelengths is the He I λ5876 emission ($v_{FWHM} \approx 2100$ km s^{-1}), possibly superposed on a less prominent, broader component ($v_{FWHM} \approx 7500$ km s^{-1}).

Other prominent and narrow (but resolved) lines are He I λ6678 and He I λ7065 ($v_{FWHM} \approx 1400-1500$ km s^{-1}). At this time, there is no evidence for the presence of a narrow Hα. The He I λ7281 emission appears to be broader than other He I lines, having $v_{FWHM} \approx 2600$ km s^{-1}, though its profile may be warped by the telluric absorption band. We may also consider the possibility of a blend with nebular emission lines at about 7300 Å, such as [Ca II] $\lambda\lambda$7291,7323 or, less likely, [O II] $\lambda\lambda$7320,7330. Other weaker He I lines identified in the optical spectra are λ3889, λ4471, λ4922 and λ5016. At longer wavelengths, we clearly note the presence of very broad emissions identified as O I at 7772-7775 Å (possibly blended with Mg II, with $v_{FWHM} \approx 10^4$ km s^{-1}), O I λ8446 and, though weaker, the NIR Ca II triplet.

The two latest spectra (obtained in March and April 2013) show a new feature at about 6300 Å, that becomes more prominent with time. We identify it as the emerging [O I] $\lambda\lambda$6300,6364 doublet typical of core-collapse SNe. In

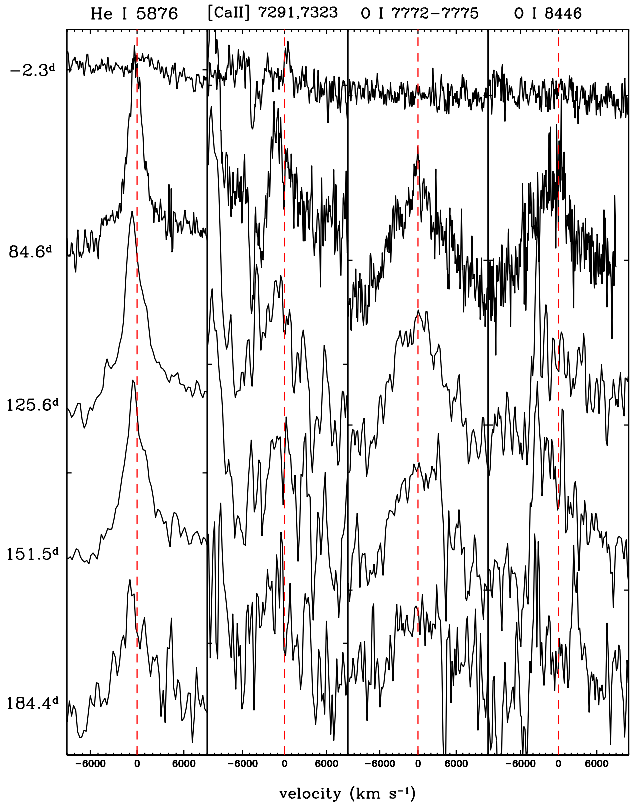

Figure 6. From the left to the right: evolution of the profiles of He I λ5876, [Ca II] $\lambda\lambda$7291,7323, the O I $\lambda\lambda$7772-7775 and O I λ8446. The numbers on the left indicate the phases of the spectra from the maximum light.

addition, in the 2013 April 19th spectrum, the 7300 Å feature has now similar strength as the He I λ7065 emission. This is probably an indication of the increased contribution of the [Ca II] $\lambda\lambda$7291,7323 (or, perhaps, [O II] $\lambda\lambda$7320,7330) component in the blend with He I λ7281. In Figure 6 we show the time evolution of the profiles of representative spectral lines in OGLE-2012-SN-006, in the velocity space: He I λ5876, the [Ca II] $\lambda\lambda$7291,7323 doublet, the O I features at 7772-7775 Å and 8446 Å. In Figure 7 late-time (3 and 6 months past maximum) spectra of OGLE-2012-SN-006 are compared with those of the Type Ib SNe 1990I and 2007C at similar phases. We note than, in contrast with that observed in late Type Ib SNe, in OGLE-2012-SN-006 the O I λ8446 line is the most prominent feature at the red wavelengths, and largely dominates over the Ca II NIR triplet.

The He I emission lines have a slightly blue-shifted peak, and the amount of blue-shift increases with time, from $\sim$ 250 km s^{-1} in the two January 2013 spectra to about 400-500 km s^{-1} in the February-March 2013 spectra (see also Figure 6, left panel). Unfortunately, the last available spectrum (April 19, 2013) has a very low signal-to-noise. However, from the position of the He I λ5876 emission, we tentatively infer a blue-shift of 700 $\pm$ 150 km s^{-1}. In addition, the emission profiles show an evident asymmetry. All of this would support our claim (Section 2.1) that some dust is forming in OGLE-2012-SN-006 at late phases. We remark that in SN 2006jc the formation of dust was observed in a post-shock cool dense shell starting from $\sim$50 days after the SN explosion (Smith et al. 2008; Mattila et al. 2008). Blue-shifted line emissions are frequently observed in late-time spectra of SNe IIn, and are usually considered a signature of dust formation (e.g. Gerardy et al. 2000; Fransson et al. 2005; Stritzinger et al. 2012). However, an evident blueshift of the broad Hα line component was observed in the Type IIn SN 2010jl (see Fransson et al. 2014, their figure 12), and was interpreted as resulting from the bulk gas velocity, likely due to acceleration of unshocked gas by the SN radiation field.

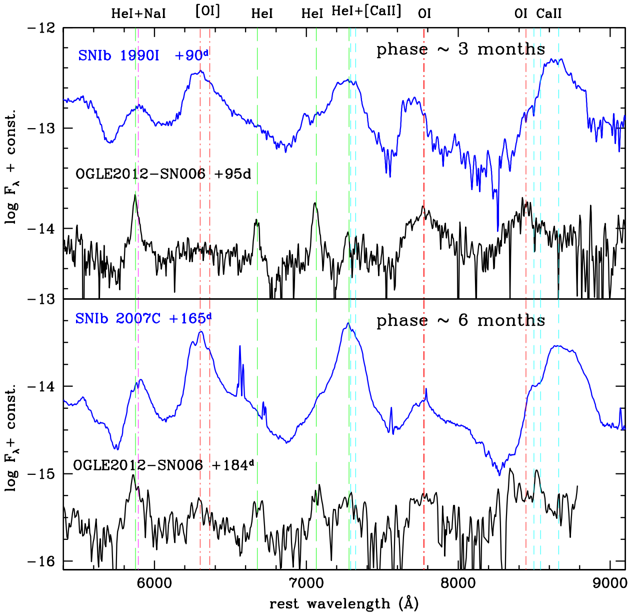

Figure 7. Top: Comparison between spectra of OGLE-2012-SN-006 and the Type Ib SN 1990I at about 3 months after maximum. Bottom: a later ($\sim$6 months) spectrum of OGLE-2012-SN-006 is compared with one of the SN Ib 2007C at a similar phase. The spectra of the comparison Type Ib SNe are from Taubenberger et al. (2013). The position of the most important lines is marked with vertical lines: He I (green colour), Na I (magenta), O I (red) and Ca II (cyan).

In Figure 8 a late-time optical + NIR spectrum of OGLE-2012-SN-006 obtained with the NTT between 2013 January 19th and 21st (at about 128 days after maximum) is compared with a VLT + XShooter spectrum of the Type Ibn SN 2010al (phase $\sim$ 44 days since light curve peak) presented in Pastorello et al. (2015a). Despite the moderate signal-to-noise, the two spectra are very similar, being dominated by prominent He I lines (marked with red dot-dashed lines in the figure). In particular, the strongest He I line is the λ10830 feature. Other He I features clearly detected in the NIR spectrum of OGLE-2012-SN-006 are the λ17002 and λ20581 lines, and a blend at around 18690 Å. We also notice the overall similarity of the two spectra in the optical domain, both showing the prominent blend formed by O I λ8446 with the NIR Ca II triplet, while the O I λ7774 feature is much stronger in the spectrum of OGLE-2012-SN-006 (although it is clearly detected also in SN 2010al).

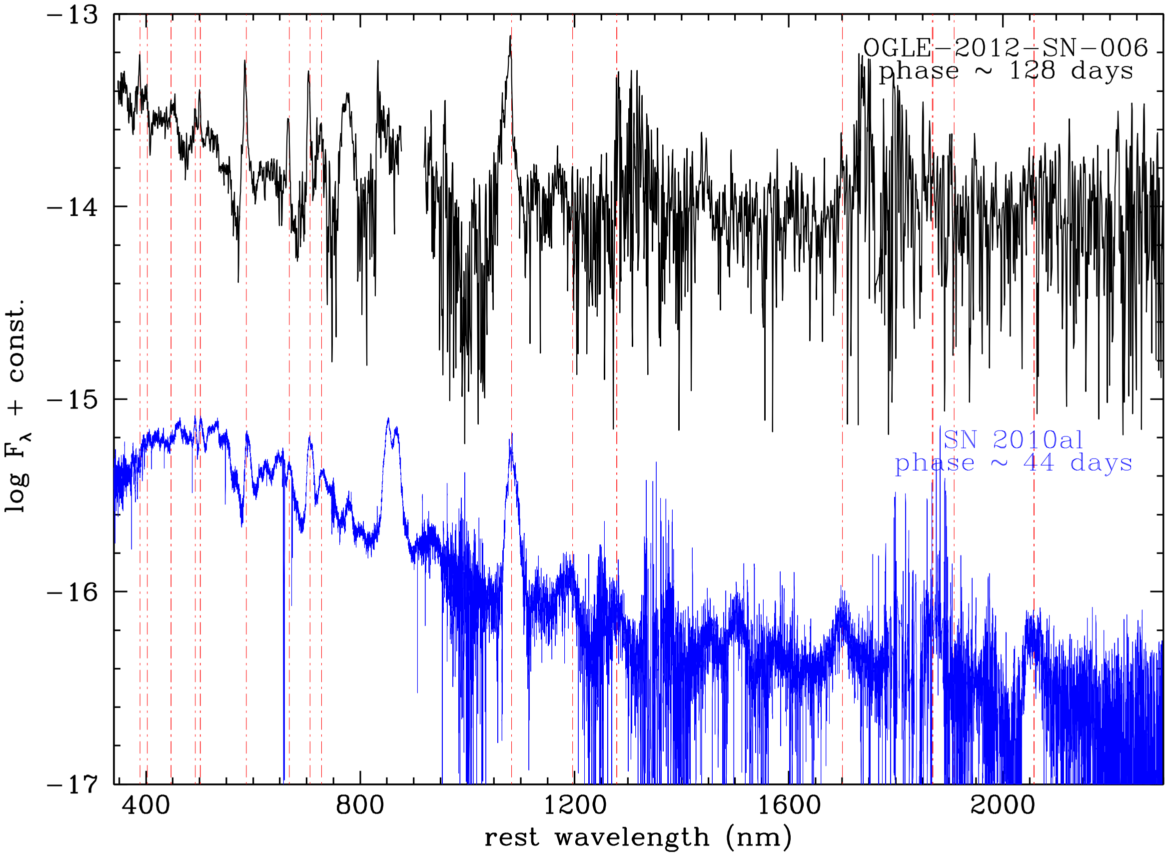

Figure 8. Optical + NIR spectrum of OGLE-2012-SN-006 (∼128 days after maximum) compared with an X-Shooter spectrum of SN 2010al (Pastorello et al. 2015b) obtained when the SN was about 44 days past maximum (i.e. 2 months after the explosion). The red dot-dashed lines mark the position of the strongest He I features. The two spectra have been redshift-corrected. Both objects show rather prominent features of O I λ7774 (much stronger in OGLE-2012-SN-006), and O I λ8446 plus the Ca II NIR triplet.

3 DISCUSSION AND SUMMARY

OGLE-2012-SN-006 is an interesting object owing to its unprecedented properties in the context of the Type Ibn SN family. An early-time spectrum shows a blue continuum and broad absorptions probably due to CNO elements (mostly O II), that are not frequently observed in classical core-collapse SN spectra. These spectral features are similar to those observed in super-luminous stripped-envelope transients (Quimby et al. 2011). The post-peak optical and NIR light curves show a fast decline until about one month after the explosion. Then the light curves level off to a very slow decline rate. In coincidence with the late curve flattening, the spectra show the relatively narrow He I in emission typical of the Type Ibn SN family, which are interpreted in terms of interaction with He-rich CSM. The late light curve tail has initially a flat slope, although later (starting from about 4 months after the explosion) it shows a decline rate similar to that expected when the powering mechanism is the radioactive decay of ^{56}Co into ^{56}Fe. The optical light curves of the prototype SN 2006jc showed a much faster decline in the optical bands and an increasing luminosity in the IR domain. This was interpreted as a signature of dust formation (Smith et al. 2008; Mattila et al. 2008; Di Carlo et al. 2008; Nozawa et al. 2008; Sakon et al. 2009) in a post-shock cool and dense circumstellar shell. However, there is evidence of an increasing slope in the late-time *I*-band light curve in OGLE-2012-SN-006, which may be attributed to dust formation also in this case.

An important issue that we have not yet discussed is the physical mechanisms that could power the bright peak luminosity and the unprecedented photometric evolution of the Type Ibn OGLE-2012-SN-006. For this goal, we have calculated a (quasi)-bolometric light curve for OGLE-2012-SN-006 by integrating the flux contribution in individual optical and NIR pass-bands. In practice, for each epoch with *I*-band observations available and for each band, we derived the flux at the effective wavelength. When photometric points in individual bands were not available at a given epoch, their contribution was estimated through an interpolation of photometry in adjacent epochs. Unfortunately, early-time photometry was available for OGLE-2012-SN-006 only in the *I* and (to a lesser extent) in the *V* band. The flux contribution of the missing bands at early phases, in particular during the rising branch to the peak and the period around maximum, has been obtained under the rough assumption that the early colour evolution of OGLE-2012-SN-006 was similar to that of the Type Ibn SN 2010al (Pastorello et al. 2015a). Although the colour evolutions of SNe 2010al and

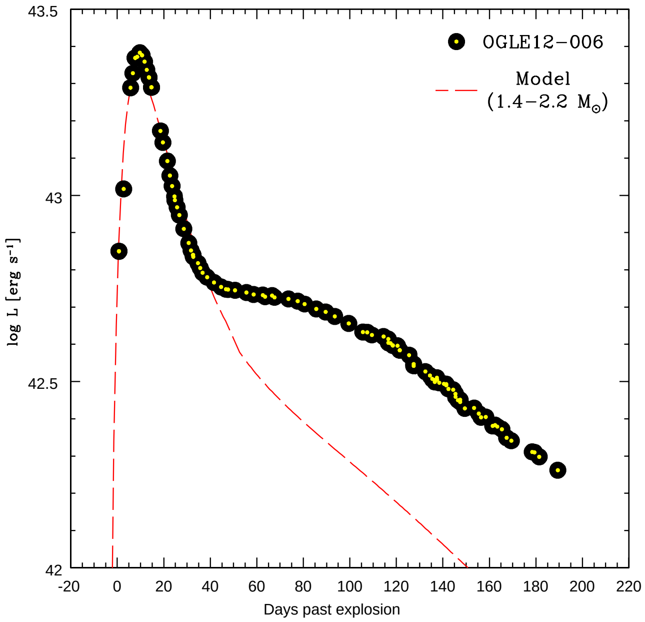

Figure 9. Comparison between the pseudo-bolometric light curve of OGLE-2012-SN-006 and a radioactively-powered light curve model. As we have limited information on the ejecta velocity at the time of the light curve peak, we assume that the photospheric velocity at maximum is v = 15000 ± 1000 km s^{-1}. We adopt an optical opacity of χ = 0.1 cm^2 g^{-1}. A model which provides a decent match with the observed quasi-bolometric light curve of OGLE-2012-SN-006 at early phases, is obtained adopting the following parameters: M(^{56}Ni) = 0.8 - 1.1 M$_\odot$, M$_{ej}$ = 1.4 - 2.2 M$_\odot$, E$_K$ = $1.3 - 7.5 \times 10^{51}$ erg. Clearly, a poor match is obtained with the late-time light curve of OGLE-2012-SN-006.

OGLE-2012-SN-006 are very different, there is a good match in the early-time optical colours (up to ∼15 days past maximum; see Figure 3, middle panel). The fluxes, corrected for the adopted extinction, provide the spectral energy distribution at the given phase, which are then integrated through the trapezoidal rule. The observed flux is finally converted to luminosity adopting the distance and interstellar reddening values mentioned above. We did not account for flux contribution beyond the observed *U* and NIR bands, and therefore this has been more properly quoted as a "quasi-bolometric" light curve. We should emphasize that the luminosity contribution of the UV domain, especially at early phases, may be significant (see e.g. Pastorello et al. 2015a). The resulting quasi-bolometric light curve is shown in Figure 9.

Although we have limited information on the spectroscopic and photometric evolution of OGLE-2012-SN-006, we attempt to constrain SN parameters using the quasi-bolometric light curve computed before, with the initial assumption that the SN luminosity peak is mostly powered by the radioactive decays. To this aim, we fit the SN data using a toy light-curve model elaborated by Valenti et al. (2008),[7] which has been shown to successfully reproduce the early-phase bolometric light curves of various stripped-envelope SNe. The model of Valenti et al. (2008) is based on simple analytical approximations (Arnett 1982; Cappellaro et al. 1997; Clocchiatti & Wheeler 1997), and on a division of the light curve into two periods. In the first period, the supernova is optically thick (photospheric phase); later on, it gets optically thin (nebular phase). The model assumes that - at least in the early phase (< 50 days) - the CSM-ejecta interaction does not provide a major contribution to the observed bolometric luminosity. By assessing the model consistency, we will make an effort to test this assumption, although it may appear natural since the early light curve of OGLE-2012-SN-006 resembles those of radioactively-powered Type Ia and/or Type Ib/c SNe, and our earliest spectrum shows no narrow emission lines from interaction. The comparison between the bolometric light curve of OGLE-2012-SN-006 and our best light curve model of a radioactively powered stripped-envelope SN is shown in Figure 9 (the parameters used for the model are illustrated in the figure caption). If the SN radiation is powered by radioactive decays, this would imply a relatively high kinetic energy and extremely small ejecta mass, a large fraction of which would be ^{56}Ni. The inferred M(^{56}Ni)/M$_{ej}$ ratio (∼0.5) is similar to those estimated in some luminous Type Ia SNe (e.g. Taubenberger et al. 2013), but are not comfortably accomodated in the context of a core-collapse explosion scenario. We also note the late-time spectra are dominated by He and α-elements, and not by iron-peak elements. All of this clearly argues against the initial assumptions adopted for the model, and suggests that the ^{56}Ni to ^{56}Co to ^{56}Fe decay chain is not the primary process which powers the light curve of OGLE-2012-SN-006. As a consequence, ejecta-CSM interaction provides a more plausible explanation.

We note, however, that a degenerate progenitor system scenario had been previously proposed by Sanders et al. (2013) for another Type Ibn SN, PS1-12sk. The unusual location of that object in the outskirts of an elliptical galaxy, suggested a progenitor scenario which could have been different from the canonical core-collapse of a massive, stripped-envelope star normally assumed for SNe Ibn, including the possibility of a white dwarf explosion in a He-rich environment (Sanders et al. 2013). However, to our knowledge, this still remains a unique case in the Type Ibn SN zoo, since all other objects exploded in spiral galaxies (Pastorello et al. 2015b). In addition, as admitted by Sanders et al. (2013), some residual star formation at the SN location and/or the association with a nearby, low luminosity dwarf galaxy cannot be ruled out, and -consequently- the progenitor may still be a massive star.

The fact that SNe Ibn explode preferentially in young stellar population environments, the pre-SN eruption detected in SN 2006jc and -even more- the detection of the [O I] $\lambda\lambda$ 6300,6364 doublet in the late spectra of OGLE-2012-SN-006, are robust arguments to support a core-collapse scenario for Type Ibn SNe. As mentioned before, the high M(^{56}Ni)/M$_{ej}$ ratio estimated for OGLE-2012-SN-006 from the model described above, can be explained with incorrect initial assumptions on the source powering the early light curve of this object. In other words, the high luminosity at peak may have not been completely due to radioactive decay. In the view of the presence of a dense He shell, we argue that other processes may give a significant contribu-

---

[7] This model is obtained using the code of Valenti et al. (2008), which is based on Arnett (1982), but accounting for the typo correction reported in Arnett (1996) - (see Wheeler et al. 2014).

tion to the total SN luminosity around maximum light. As a consequence, the assumptions from using the toy model are violated, and the progenitor and explosion parameters are likely to be significantly different from those derived in the simple model fits. Almost certainly the explosion of OGLE-2012-SN-006 produced a smaller amount of ^{56}Ni and a larger ejecta mass.

In this context, there is an appealing qualitative similarity between the quasi-bolometric light curve of OGLE-2012-SN-006 and the light curve models discussed in Falk & Arnett (1977). In particular, there is a surprising match with the light curve models obtained considering a stellar ejected envelope plus an overlying circumstellar shell (Models B of Falk & Arnett 1977, see e.g. their figure 10). According to these models, the luminous peak would be the result of radiative heating and diffusion of radiation ahead of the shock front in a low-density circumstellar shell. Modern simulations of this class of interaction-powered SNe have been presented in detail, for example, by Moriya et al. (2011). According to Moriya & Tominaga (2012) the absence of prominent narrow lines, as in the case of the early spectrum of OGLE-2012-SN-006, would not be an indication of lack of interaction. Instead, it could be related with a non-steady mass loss of the progenitor prior to the explosion. Although this scenario was used to explain the early behavior of H-rich SNe, it might be extended to Type I events, such as OGLE-2012-SN-006. However, while in the case of the models of Falk & Arnett (1977) or Moriya et al. (2011) the H envelope recombination sets the post-peak luminosity evolution, in SNe Ibn the ejecta-CSM interaction is probably the preponderant source of energy powering the light curve until late phases.

The precursors of Type Ibn SNe have been proposed to be H-depleted, He-rich (i.e. “WN” type, Foley et al. 2007) Wolf-Rayet (WR) stars or more He-poor (of “WC-O” type, Pastorello et al. 2007; Tominaga et al. 2008) WR stars. In addition, a few rare and moderately H-rich Ibn events, such as SNe 2005la and 2011hw, have been proposed to be produced by stars that were transiting from luminous blue variable to WR stages (e.g. WN-type, Smith et al. 2012; Pastorello et al. 2015a). In this context, the spectra of OGLE-2012-SN-006 show very little evidence for the presence of H lines (and only in the first spectrum), thus suggesting that the precursor was an almost totally H-depleted WR star that suffered major mass loss processes before exploding as a core-collapse SN.

So far, we have collected incomplete information from an increasing number of Type Ibn SNe. In order to increase our knowledge on this SN family, we need to promptly detect a young SN Ibn just after explosion, and follow it until the nebular phase. With OGLE-2012-SN-006, we partly reached that aim, since we collected valuable information on the evolution of a SN Ibn until very late phases. However, because of the slow reaction of the astronomical community and the unusual properties of the early-time spectrum, it was not promptly classified. As a consequence, we missed the opportunity to better sample the impressive spectral metamorphosis at early times that can be only inferred from the available data. In addition, we did not target OGLE-2012-SN-006 in the ultra-violet (UV) domain, which is crucial to properly estimate the UV contribution to the total luminosity during the first few days after the explosion. An efficient cooperation and exchange of information within the astronomical community is essential to achieve these goals, and we aim to do this as soon as a new suitable young SN Ibn will become available.

ACKNOWLEDGMENTS

We would like to thank the anonymous referee for providing us with constructive comments and suggestions.

AP, EC, SB and MT are partially supported by the PRIN-INAF 2011 with the project *”Transient Universe: from ESO Large to PESSTO”*. NER acknowledges the support from the European Union Seventh Framework Programme (FP7/2007-2013) under grant agreement n 267251 Astronomy Fellowships in Italy (AstroFIt). AMG acknowledges financial support by the MICINN grant AYA2011-24704/ESP, by the ESF EUROCORES Program EuroGENESIS (MINECO grants EUI2009-04170), SGR grants of the Generalitat de Catalunya and by the EU-FEDER funds. SS acknowledges support from CONICYT-Chile FONDECYT 3140534, Basal-CATA PFB-06/2007, and Project IC120009 ”Millennium Institute of Astrophysics (MAS)” of Iniciativa Científica Milenio del Ministerio de Economía, Fomento y Turismo.

Research leading to these results has received funding from the European Research Council under the European Union s Seventh Framework Programme (FP7/2007-2013)/ERC Grant agreement no. [291222] (PI: SJS) and EU/FP7-ERC grant no. [307260] (PI: AG-Y). AG-Y is also supported by The Quantum Universee I-Core programme by the Israeli Committee for planning and funding and the ISF, a GIF grant, and the Kimmel award. The OGLE project has received funding from the European Research Council under the European Communitys Seventh Framework Programme (FP7/2007- 2013)/ERC grant agreement no. 246678 to AU. This work is partially supported by the Polish Ministry of Science and Higher Education program ”Ideas Plus” No. IdP2012 000162, and is also partly supported by the European Union FP7 programme through ERC grant number 320360

This paper is partially based on observations obtained under the ESO-NTT Large Program 188.D-3003 (the Public ESO Spectroscopic Survey for Transient Objects - *PESSTO*). This work makes use of observations from the LCOGT network, the 1.3m Warsaw university Telescope and the 2.5m du Pont Telescope at the Las Campanas Observatory, the 2.2m MPI/ESO Telescope and the 3.58m ESO New Technology Telescope at ESO-La Silla.

We thank Jonathan Elliott (MPE Garching) for executing the GROND observation. AP thanks M. L. Pumo for useful discussions. Part of the funding for GROND (both hardware as well as personnel) was generously granted from the Leibniz-Prize to Prof. G. Hasinger (DFG grant HA 1850/28-1).

This publication makes use of data products from the Two Micron All Sky Survey, which is a joint project of the University of Massachusetts and the Infrared Processing and Analysis Center/California Institute of Technology, funded by the National Aeronautics and Space Administration and the National Science Foundation. This research has made use of the NASA/IPAC Extragalactic

Database (NED) which is operated by the Jet Propulsion Laboratory, California Institute of Technology, under contract with the National Aeronautics and Space Administration. We acknowledge the usage of the HyperLeda database (http://leda.univ-lyon1.fr).

REFERENCES

Anupama, G. C., Sahu, D. K., Gurugubelli, U. K., Prabhu, T. P., Tominaga, N., Tanaka, M., Nomoto, K. 2009, MNRAS, 392, 894

Arnett W. D., 1982, ApJ, 253, 785

Arnett, W. D. 1996, in *Supernovae and Nucleosynthesis: An Investigation of the History of Matter, from the Big Bang to the Present*, by D. Arnett. Princeton: Princeton University Press

Cappellaro E., Mazzali P. A., Benetti S., Danziger I. J., Turatto M., della Valle M., Patat F. 1997, A&A, 328, 203

Chugai, N. N. 2009, MNRAS, 400, 866

Clocchiatti A., Wheeler J. C. 1997, ApJ, 491, 375

Di Carlo, E. et al. 2008, ApJ, 684, 471

Falk, S. W., Arnett, W. D. 1977, ApJS, 33, 151

Fisher, A. 2000, PhD Thesis, University of Oklahoma

Foley, R. J. et al. 2007, ApJ, 657, L105

Fransson et al. 2014, MNRAS, 797, 118

Fransson et al. 2005, ApJ, 622, 991

Gerardy, C. L., Fesen, R. A., Höflich, P., Wheeler, J. C. 2000, AJ, 119, 2968

Gorbikov et al. 2014, MNRAS, 443, 671

Greiner et al. 2008, PASP, 120, 405

Kozłowski, S. et al. 2013, Acta Astron., 63, 1

Landolt, A. U. 1992, AJ, 104, 340

Mattila, S. et al. 2008, MNRAS, 389, 141

Modjaz, M. et al. 2009, ApJ, 702, 226

Moriya, T. et al. 2011, MNRAS, 415, 199

Moriya, T. J., Tominaga, N. 2012, ApJ, 747, 118

Nakano, S., Itagaki, K., Puckett, T., Gorelli, R. 2006, CBET, 666, 1

Nozawa, T. et al. 2008, ApJ, 684, 1343

Paczynski, B. 1986, ApJ, 304, 1

Paczynski, B. 1991, ApJ, 371, L63

Pastorello, A. et al. 2007, Nature, 447, 829

Pastorello, A. et al. 2008a, MNRAS, 389, 113

Pastorello, A. et al. 2008b, MNRAS, 389, 131

Pastorello, A. et al. 2010, ApJL, 724, 16

Pastorello, A. et al. 2015a, accepted (eprint arXiv: submit/1186154)

Pastorello, A. et al. 2015b, accepted (eprint arXiv: submit/1186334)

Prieto, J. L., Morrell, N. 2012, Astron. Tel. 4734, 1

Quimby, R. M., Aldering, G., Wheeler, J. C., Höflich, P., Akerlof, C. W., Rykoff, E. S. 2007, ApJL, 668, 99

Quimby, R. M. et al. 2011, Nature, 474, 487

Sakon, I. et al. 2009, ApJ, 692, 546

Sanders, N. E. et al. 2013, ApJ, 769, 39

Schlafly, E. F., Finkbeiner D. P. 2011, ApJ, 737, 103

Skrutskie, M. F. et al. 2006, AJ, 131, 1163

Smartt, S. J. et al. 2013, The Messenger, 154, 50

Smith, N., Foley, R. J., Filippenko, A. V. 2008, ApJ, 680, 568

Smith, N. et al. 2009, ApJ, 695, 1334

Smith, N. et al. 2012, MNRAS, 426, 1905

Stoll, R. et al. 2011, ApJ, 730, 34

Stritzinger, M. et al. 2012, ApJ, 756, 173

Taubenberger, S. et al. 2013, MNRAS, 432, 3117

Tominaga, N. et al. 2008, ApJ, 687, 1208

Valenti S. et al. 2008, MNRAS, 383, 1485

Udalski, A., Kubiak M., Szymański, M. 1997, Acta Astron., 47, 319

Wheeler, J. C, Johnson, V., Clocchiatti, A. 2014, MNRAS, submitted (eprint arXiv:1411.5975)

Woźniak, P. R. 2000, Acta Astron., 50, 421

Wyrzykowski, Ł., Udalski, A., Kozłowski, S. 2012, Astron. Tel. 4495, 1

Wyrzykowski, Ł. et al. 2014, Acta Astronomica, submitted

Yamaoka, H., Nakano, S., Itagaki, K. 2006, CBET, 666, 2

Yaron, O., Gal-Yam, A. 2012, PASP, 124, 668

Zhang, T. et al. 2012, AJ, 144, 131

APPENDIX A: PHOTOMETRY OF OGLE-2012-SN-006

Table A1: Optical photometry of OGLE-2012-SN-006.

Date (dd/mm/yy)	JD (+2400000)	U	B	V	R	I	Instrument
03/07/12	56111.92	-	-	-	-	> 21.16	1
16/07/12	56124.93	-	-	-	-	> 22.29	1
11/08/12	56150.88	-	-	-	-	> 22.93	1
20/08/12	56159.91	-	-	-	-	> 22.97	1
27/08/12	56166.87	-	-	-	-	> 22.55	1
01/09/12	56171.84	-	-	-	-	> 22.77	1
20/09/12	56190.88	-	-	-	-	> 23.79	1
21/09/12	56191.86	-	-	-	-	> 23.87	1
29/09/12	56199.76	-	-	-	-	> 22.68	1
07/10/12	56207.84	-	-	-	-	18.99 (0.06)	1
09/10/12	56209.84	-	-	-	-	18.52 (0.06)	1
12/10/12	56212.81	-	-	-	-	17.65 (0.02)	1
13/10/12	56213.83	-	-	-	-	17.59 (0.03)	1
14/10/12	56214.82	-	-	17.69 (0.03)	-	17.47 (0.02)	1
15/10/12	56215.69	-	-	-	-	17.46 (0.02)	1
16/10/12	56216.81	-	-	-	-	17.39 (0.02)	1
17/10/12	56217.75	-	-	-	-	17.39 (0.02)	1
18/10/12	56218.85	-	-	-	-	17.41 (0.02)	1
19/10/12	56219.76	-	-	-	-	17.45 (0.02)	1
20/10/12	56220.70	-	-	-	-	17.47 (0.02)	1
20/10/12	56220.82	-	-	-	-	17.47 (0.02)	1
21/10/12	56221.80	-	-	17.92 (0.03)	-	17.52 (0.02)	1
25/10/12	56225.69	-	-	-	-	17.70 (0.02)	1
26/10/12	56226.70	-	-	-	-	17.76 (0.03)	1
28/10/12	56228.66	-	-	-	-	17.79 (0.04)	1
29/10/12	56229.70	-	-	-	-	17.92 (0.03)	1
30/10/12	56230.69	-	-	-	-	17.96 (0.03)	1
31/10/12	56231.71	-	-	-	-	18.01 (0.03)	1
31/10/12	56231.87	-	19.31 (0.10)	18.77 (0.08)	18.50 (0.04)	18.06 (0.06)	2
01/11/12	56232.80	-	-	-	-	18.09 (0.03)	1
02/11/12	56233.77	-	-	-	-	18.15 (0.03)	1
04/11/12	56235.75	-	-	-	-	18.19 (0.03)	1
06/11/12	56237.82	-	-	-	-	18.24 (0.03)	1
07/11/12	56238.79	-	-	-	-	18.34 (0.03)	1
08/11/12	56239.69	-	-	-	-	18.39 (0.03)	1
08/11/12	56239.78	-	-	-	-	18.44 (0.03)	1
10/11/12	56241.77	-	-	-	-	18.38 (0.04)	1
11/11/12	56242.78	-	-	-	-	18.43 (0.03)	1
12/11/12	56243.79	-	-	-	-	18.50 (0.03)	1
14/11/12	56245.77	-	-	20.04 (0.05)	-	18.54 (0.03)	1
17/11/12	56248.70	-	-	-	-	18.55 (0.03)	1
20/11/12	56251.72	-	-	-	-	18.59 (0.03)	1
22/11/12	56253.82	-	-	20.01 (0.10)	19.53 (0.09)	-	3
22/11/12	56253.83	-	-	20.00 (0.06)	-	-	3
23/11/12	56254.72	-	-	-	-	18.60 (0.03)	1
26/11/12	56257.73	-	-	-	-	18.59 (0.04)	1
01/12/12	56262.65	-	-	-	-	18.64 (0.04)	1
04/12/12	56265.71	-	-	-	-	18.68 (0.03)	1
06/12/12	56267.65	-	-	20.14 (0.06)	-	-	1
08/12/12	56269.67	-	-	20.20 (0.05)	-	18.63 (0.03)	1
09/12/12	56270.65	-	-	-	-	18.69 (0.03)	1
12/12/12	56273.67	-	-	20.08 (0.06)	-	18.63 (0.03)	1
13/12/12	56274.71	-	-	-	-	18.69 (0.03)	1
19/12/12	56280.72	-	-	-	-	18.68 (0.04)	1
23/12/12	56284.69	-	-	-	-	18.69 (0.04)	1
26/12/12	56287.64	-	-	-	-	18.73 (0.04)	1
31/12/12	56292.65	-	-	-	-	18.80 (0.04)	1

Table A1: continued.

Date (dd/mm/yy)	JD (+2400000)	*U*	*B*	*V*	*R*	*I*	Instrument
04/01/13	56296.69	-	-	-	-	18.78 (0.04)	1
08/01/13	56300.63	-	-	-	-	18.84 (0.04)	1
14/01/13	56306.62	-	-	-	-	18.93 (0.04)	1
20/01/13	56312.70	19.79 (0.11)	20.58 (0.03)	20.15 (0.03)	19.84 (0.03)	19.03 (0.05)	3
22/01/13	56314.59	-	-	-	-	19.01 (0.05)	1
24/01/13	56316.59	-	20.59 (0.36)	20.04 (0.21)	19.80 (0.21)	19.12 (0.26)	4
26/01/13	56318.59	-	-	19.98 (0.12)	19.78 (0.11)	-	4
27/01/13	56319.59	-	-	20.00 (0.08)	19.76 (0.09)	-	4
29/01/13	56321.59	-	-	-	-	19.02 (0.05)	1
29/01/13	56321.59	-	-	20.02 (0.12)	19.79 (0.11)	-	4
31/01/13	56323.59	-	-	20.11 (0.05)	19.66 (0.11)	-	4
31/01/13	56323.62	-	-	-	-	18.94 (0.04)	1
31/01/13	56323.67	19.86 (0.09)	20.55 (0.10)	20.15 (0.03)	19.83 (0.06)	19.07 (0.04)	3
31/01/13	56323.68	19.86 (0.09)	20.58 (0.05)	-	-	-	3
01/02/13	56324.58	-	-	-	-	19.03 (0.05)	1
02/02/13	56325.55	-	-	20.26 (0.05)	-	19.09 (0.04)	1
02/02/13	56325.60	-	-	20.06 (0.06)	19.70 (0.08)	19.10 (0.23)	4
03/02/13	56326.60	-	-	19.99 (0.10)	19.73 (0.21)	-	4
04/02/13	56327.58	-	-	20.06 (0.07)	19.60 (0.07)	19.00 (0.10)	4
05/02/13	56328.55	-	-	20.01 (0.06)	-	19.05 (0.05)	1
05/02/13	56328.58	-	-	20.01 (0.15)	19.75 (0.06)	19.07 (0.06)	4
09/02/13	56332.58	-	-	20.08 (0.22)	19.59 (0.10)	19.01 (0.06)	4
11/02/13	56334.58	-	-	-	-	19.10 (0.05)	1
11/02/13	56334.58	-	-	20.12 (0.10)	19.87 (0.05)	19.19 (0.06)	4
14/02/13	56337.54	-	-	20.03 (0.05)	19.75 (0.08)	-	4
16/02/13	56339.55	-	-	-	-	19.11 (0.05)	1
18/02/13	56341.54	-	-	20.22 (0.01)	19.98 (0.08)	19.10 (0.10)	4
19/02/13	56342.53	-	-	20.10 (0.09)	19.84 (0.01)	19.30 (0.04)	4
20/02/13	56343.53	-	-	20.17 (0.02)	19.87 (0.13)	19.22 (0.03)	4
20/02/13	56343.62	19.86 (0.10)	20.75 (0.11)	20.29 (0.07)	19.99 (0.06)	19.19 (0.05)	3
21/02/13	56344.53	-	-	20.17 (0.02)	19.85 (0.05)	19.10 (0.03)	4
21/02/13	56344.57	-	-	-	-	19.14 (0.04)	1
22/02/13	56345.53	-	-	20.11 (0.03)	19.97 (0.05)	19.20 (0.02)	4
23/02/13	56346.53	-	-	20.10 (0.08)	20.01 (0.35)	-	4
24/02/13	56347.53	-	-	19.96 (0.03)	19.89 (0.13)	19.24 (0.22)	4
25/02/13	56348.53	-	-	20.00 (0.01)	19.86 (0.08)	19.23 (0.03)	4
25/02/13	56348.55	-	-	-	-	19.17 (0.07)	1
26/02/13	56349.53	-	-	20.09 (0.02)	19.96 (0.02)	19.23 (0.03)	4
28/02/13	56351.51	-	-	20.18 (0.15)	-	19.14 (0.07)	1
01/03/13	56352.53	-	-	20.07 (0.03)	20.00 (0.03)	19.25 (0.03)	4
01/03/13	56352.55	-	-	-	-	19.35 (0.08)	1
02/03/13	56353.56	-	-	-	-	19.36 (0.07)	1
03/03/13	56354.53	-	-	-	-	19.22 (0.07)	1
03/03/13	56354.53	19.96 (0.04)	20.78 (0.04)	20.32 (0.03)	20.02 (0.03)	19.32 (0.02)	3
05/03/13	56356.53	-	-	20.29 (0.01)	20.09 (0.01)	19.45 (0.11)	4
09/03/13	56360.53	-	-	20.23 (0.05)	20.02 (0.01)	19.24 (0.03)	4
11/03/13	56362.52	-	-	-	-	19.33 (0.06)	1
12/03/13	56363.50	-	-	-	-	19.42 (0.13)	1
14/03/13	56365.53	-	-	20.24 (0.02)	19.97 (0.05)	19.34 (0.03)	5
17/03/13	56368.50	-	-	-	-	19.43 (0.08)	1
17/03/13	56368.57	20.14 (0.07)	20.88 (0.09)	20.45 (0.09)	-	-	3
18/03/13	56369.54	-	-	-	-	19.36 (0.05)	1
19/03/13	56370.50	-	-	-	-	19.36 (0.11)	1
20/03/13	56372.49	-	-	-	-	19.38 (0.09)	1
23/03/13	56374.51	-	-	-	-	19.62 (0.09)	1
25/03/13	56376.51	-	-	-	-	19.64 (0.13)	1

Table A1: continued.

Date (dd/mm/yy)	JD (+2400000)	U	B	V	R	I	Instrument
03/04/13	56385.51	20.37 (0.04)	21.08 (0.05)	20.65 (0.04)	20.36 (0.04)	19.69 (0.03)	3
03/04/13	56386.49	-	-	-	-	19.64 (0.09)	1
06/04/13	56388.51	20.40 (0.10)	21.12 (0.09)	20.69 (0.06)	20.42 (0.04)	19.73 (0.05)	3
14/04/13	56396.50	-	21.32 (0.10)	20.81 (0.05)	20.50 (0.05)	19.80 (0.09)	3
18/04/13	56401.49	20.74 (0.16)	-	-	-	-	3
19/04/13	56402.48	-	-	20.98 (0.20)	-	-	3
01/08/13	56505.90	-	-	-	-	21.86 (0.55)	1
10/08/13	56514.85	-	-	-	-	> 22.85	1
17/08/13	56521.80	-	-	-	-	> 23.04	1
20/08/13	56524.88	-	-	-	-	> 22.71	1

1 = 1.3m Warsaw University Telescope + OGLE-IV mosaic camera (Las Campanas Observatory); 2 = 2.2m MPI/ESO Telescope + GROND (ESO-La Silla Observatory); 3 = 3.58m New Technology Telescope + EFOSC2 (ESO-La Silla Observatory); 4 = LCOGT 1.0m-05 telescope + SBIG STX-16083 with Kodak KAF-16803 FI (Cerro Tololo Inter-American Observatory); 5 = LCOGT 1.0m-09 telescope + SBIG STX-16083 with Kodak KAF-16803 FI (Cerro Tololo Inter-American Observatory).

Table A2. Near-infrared photometry of OGLE-2012-SN-006.

Date (dd/mm/yy)	JD (+2400000)	*J*	*H*	*K*	Instrument
31/10/12	56231.87	16.82 (0.06)	15.77 (0.06)	15.02 (0.08)	1
29/01/13	56321.57	17.62 (0.06)	16.54 (0.05)	15.50 (0.07)	2
08/02/13	56331.61	17.81 (0.09)	-	-	2
22/02/13	56345.73	17.92 (0.08)	17.14 (0.18)	15.96 (0.11)	2
13/03/13	56364.51	18.18 (0.07)	17.62 (0.10)	16.23 (0.08)	2
12/04/13	56394.51	18.50 (0.10)	17.70 (0.11)	16.41 (0.09)	2
18/04/13	56400.53	18.51 (0.06)	17.68 (0.07)	16.43 (0.07)	2

1 = 2.2m MPI/ESO Telescope + GROND (ESO-La Silla Observatory);
2 = 3.58m New Technology Telescope + SOFI (ESO-La Silla Observatory).

Table A3. Magnitudes of the sequence stars in the field of OGLE-2012-SN-006. For the optical bands, errors in brackets are the r.m.s. of the magnitudes obtained averaging estimates obtained in photometric nights. The NIR magnitudes and the associated errors are those reported in the 2MASS catalogue (Skrutskie et al. 2006).

Star	*U*	*B*	*V*	*R*	*I*	*J*	*H*	*K*
1	20.784 (0.035)	19.282 (0.021)	17.515 (0.012)	16.195 (0.010)	14.518 (0.020)	12.919 (0.027)	12.338 (0.022)	11.983 (0.019)
2	20.446 (0.025)	20.220 (0.059)	19.417 (0.014)	18.979 (0.012)	18.523 (0.023)	-	-	-
3	18.712 (0.030)	18.848 (0.011)	18.129 (0.005)	17.709 (0.007)	17.298 (0.017)	-	-	-
4	17.637 (0.064)	17.172 (0.172)	16.289 (0.004)	15.789 (0.008)	15.358 (0.021)	14.800 (0.047)	14.313 (0.053)	14.243 (0.088)
5	-	20.322 (0.020)	18.525 (0.004)	17.324 (0.011)	15.682 (0.056)	14.262 (0.032)	13.634 (0.035)	13.390 (0.038)
6	-	20.464 (0.045)	18.827 (0.017)	17.572 (0.040)	16.112 (0.049)	14.489 (0.048)	13.830 (0.058)	13.480 (0.125)
7	18.429 (0.023)	17.127 (0.013)	15.620 (0.004)	14.699 (0.007)	13.705 (0.050)	12.650 (0.027)	11.949 (0.023)	11.762 (0.026)
8	20.746 (0.040)	19.329 (0.021)	17.779 (0.006)	16.782 (0.009)	15.630 (0.031)	14.458 (0.029)	13.791 (0.033)	13.620 (0.048)
9	21.164 (0.023)	19.936 (0.017)	18.355 (0.008)	17.281 (0.009)	15.925 (0.022)	14.668 (0.045)	14.115 (0.048)	13.729 (0.061)
10	21.419 (0.055)	19.989 (0.017)	18.411 (0.004)	17.496 (0.009)	16.534 (0.034)	15.512 (0.067)	14.916 (0.074)	14.536 (0.108)
11	21.577 (0.072)	20.554 (0.018)	18.998 (0.006)	18.089 (0.024)	17.147 (0.026)	15.997 (0.115)	15.312 (0.116)	15.075 (0.176)
12	-	21.546 (0.051)	20.086 (0.015)	19.159 (0.037)	18.239 (0.025)	-	-	-
13	-	-	21.393 (0.046)	20.286 (0.064)	19.108 (0.110)	-	-	-
14	-	21.636 (0.020)	20.241 (0.006)	19.318 (0.021)	18.530 (0.047)	-	-	-
15	-	-	21.983 (0.097)	21.084 (0.048)	20.258 (0.027)	-	-	-
16	16.899 (0.022)	16.477 (0.007)	15.621 (0.005)	15.159 (0.008)	14.723 (0.022)	14.116 (0.045)	13.744 (0.036)	13.616 (0.048)
17	18.908 (0.028)	17.739 (0.009)	16.600 (0.004)	15.926 (0.009)	15.359 (0.022)	14.588 (0.039)	14.045 (0.039)	13.823 (0.060)
18	20.246 (0.077)	20.504 (0.017)	19.852 (0.019)	19.455 (0.022)	19.070 (0.029)	-	-	-
19	-	-	21.135 (0.029)	20.587 (0.030)	20.076 (0.043)	-	-	-
20	18.925 (0.069)	18.909 (0.017)	18.493 (0.006)	18.241 (0.007)	18.022 (0.050)	-	-	-
21	17.614 (0.028)	17.417 (0.016)	16.590 (0.004)	16.135 (0.011)	15.716 (0.022)	15.172 (0.058)	14.934 (0.086)	14.414 (0.093)
22	21.755 (0.166)	20.450 (0.028)	18.882 (0.012)	17.770 (0.010)	16.352 (0.056)	15.026 (0.055)	14.295 (0.052)	14.173 (0.072)
23	15.584 (0.062)	15.128 (0.013)	14.215 (0.005)	13.745 (0.009)	13.351 (0.026)	12.770 (0.029)	12.371 (0.023)	12.278 (0.026)